

Scrambled Direct-Sequence Spread-Spectrum Underwater Acoustic Communication System

Peng Chen

School EECMS
Curtin University
Bentley, WA, Australia
peng.chen@curtin.edu.au

Yue Rong

School EECMS
Curtin University
Bentley, WA, Australia
y.rong@curtin.edu.au

Alec Duncan

CMST
Curtin University
Bentley, WA, Australia
a.j.duncan@curtin.edu.au

Abstract—This paper presents the system design of a frame-wide scrambling based direct-sequence spread-spectrum underwater acoustic communication system. To increase the data rate, in this system, multiple data streams (together with the pilot stream) are transmitted simultaneously through the channel while occupying the same frequency band. The signal processing at the transmitter and receiver is presented. In particular, an extended Kalman filter based automatic frequency offset controller is developed to track the Doppler-induced frequency offset. The bit-error-rate performance of the system is studied through numerical simulations. The simulation results indicate that with the pilot-based channel estimation, the system is reliable to transmit multiple data streams in parallel. The system works well even when the channel delay spread is longer than the spreading code duration, thanks to the important contributions of the packet-wide scrambling structure and the automatic frequency offset controller.

Keywords- Direct-sequence spread-spectrum, extended Kalman filter, underwater acoustic communication.

I. INTRODUCTION

To mitigate the large path loss in long-range underwater acoustic communication, the Direct-Sequence Spread-Spectrum (DSSS)-based technique is widely adopted for its robustness at low Signal-to-Noise Ratio (SNR) [1]. In a DSSS system, predefined code sequences are used to spread the information-bearing symbols in frequency [2]. At the transmitter, the spreading operation is performed by transmitting one information symbol through the multiple chips of a spreading sequence. The despreading processing is carried out at the receiver to harvest energy carried by every single chip of the spreading sequence to extract the information symbol. It is reported that a DSSS system has the capability to decode signals which are much weaker than the ambient noise [3], [4].

One of the challenges for applying the DSSS technique in underwater acoustic communication is the long-delay multipath [5]. This may lead to severe interchip and intersymbol interference in the received signal. To mitigate this distortion,

the spreading sequence should be as orthogonal to any of its cyclically shifted versions as possible.

Receiver designs for underwater acoustic DSSS communications have been presented in the literature. In [4], [6], [7], non-coherent cross-correlation and energy-detection based receivers have been demonstrated for dynamic ocean environments. This type of receiver suffers from low data rate and is usually adopted for extremely low SNR scenarios where proper channel estimation is almost impossible.

The rake receiver, which achieves multipath diversity by combining the signal energy from multiple paths, is another despreading solution in DSSS underwater acoustic communication [8], [9]. This kind of receiver is phase-coherent, thus it requires a higher SNR compared with the non-coherent solutions. DSSS systems with the rake receiver can achieve a higher data rate as Quadrature Phase-Shift Keying (QPSK) and Quadrature Amplitude Modulation (QAM) constellations can be utilized. Decision Feedback Equalizer (DFE) based receiver is another phase-coherent despreading approach to eliminate severe interchip and intersymbol interference. It has been successfully applied in [10]-[12] on the symbol or chip level to suppress multipath interference and achieve processing gain. In [13], the performance of the rake receiver for weak signals is compared with the DFE receiver for underwater communication applications.

Another challenge for DSSS systems is the large and time-varying frequency offset caused by the Doppler effect and the frequency instability of the receiver local oscillator. The classical approach to cope with frequency offset and its time variation is an analog second-order or higher order phase-locked loop (PLL) [14]. Other schemes have been developed to combat frequency offset, such as the dual-pilot tone calibration approach [15] and the demodulation method [16]. The disadvantage of the technique in [15] is its low efficiency as it requires a long preamble. The method in [16] uses the discrete Fourier transform to estimate the carrier frequency in the frequency domain. Since this method needs to store digital signals, its



computational complexity and required memory grow fast with the data length used to perform estimation.

The slow speed of sound results in relatively large Doppler shifts compared with those normally experienced by radio signals. The wideband feature of acoustic signals limits the techniques that can be used for mitigating the Doppler shifts. A two-step Doppler frequency control scheme is widely adopted by the underwater acoustic communication community to mitigate the impact of large Doppler frequency on wideband signals [17]. In the first step, a coarse estimate of the Doppler shift is obtained from the preamble and/or postamble, and the received signals are resampled based on the estimated Doppler shift. In the second step, the frequency offset in the user data packet is removed by using automatic frequency control algorithms designed for narrow-band signals.

This paper presents the system design of a frame-wide scrambling based DSSS underwater acoustic communication system. To increase the data rate, in this system, multiple data streams (together with the pilot stream) are transmitted simultaneously through the channel while occupying the same frequency band. A unique spreading sequence is assigned to each data stream and the pilot stream.

State-of-the-art DSSS systems use m-sequence or binary Zero Correlation Zone (ZCZ) sequence as spreading codes and require that the channel delay spread is shorter than the spreading code duration [10], [18]. However, this assumption does not hold for underwater acoustic channels with a long delay spread. To overcome this challenge, we utilize Walsh sequences as spreading codes and a packet-wide scrambling process is adopted after stream combining. Scrambling after spreading is widely used in terrestrial communication systems (IS95, WCDMA, CDMA2000, etc.) to separate users or base stations. However, in this paper this technology is used to estimate long-delay channels.

The signal processing at the transmitter and receiver is presented in this paper. In particular, an Extended Kalman Filter (EKF) based automatic frequency offset controller is developed to track the Doppler-induced frequency offset. The Bit-Error-Rate (BER) performance of the DSSS system is studied through numerical simulations. The simulation results indicate that with the pilot-based channel estimation, the system is reliable to transmit multiple data streams in parallel. The system works well even when the channel delay spread is longer than the spreading code duration, thanks to the important contributions of the packet-wide scrambling structure and the automatic frequency offset controller.

The remainder of this paper is organized as follows. The transmitter and receiver design is presented in Section II. Numerical simulation results are demonstrated in Section III. In Section IV, conclusions are drawn.

II. SYSTEM DESIGN

A. Transmitter

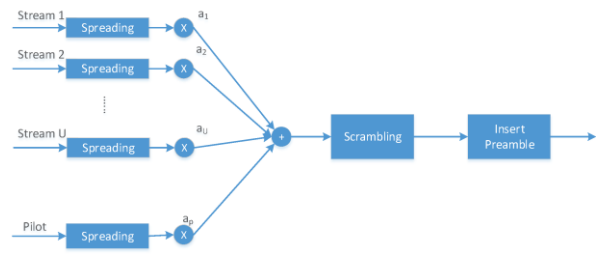


Figure 1. Transmitter block diagram of the DSSS system.



Figure 2. Data packet structure of the DSSS system.



Figure 3. Receiver block diagram of the DSSS system.

Fig. 1 shows the transmitter structure of the DSSS communication system, where U data streams are transmitted in parallel, together with the pilot stream. Each symbol in the data and pilot streams is first spread by a unique L_w -chip Walsh code sequence assigned to this stream and then multiplied with a predetermined factor to scale its energy. The data streams and the pilot stream are combined after the spreading and scaling operations.

The packet payload consists of N_d symbols and the scrambling operation is performed on the payload. Note that the length of the scrambling sequence is identical to the number of chips in a packet payload. Finally, a preamble is inserted into the packet for packet detection and/or channel estimation. The preamble consists of an L_{pr} -chip sequence. The n th transmitted chip of the payload is presented as

$$x[n] = \left(\sum_{u=1}^U \alpha_u S_u[m_s] W_u[m_w] + \alpha_p S_p[m_s] W_p[m_w] \right) C[n] \quad (1)$$

where α_u is the scaling factor of the u th stream, $C[n]$ is the n th chip of the scrambling sequence, $W_u[m_w]$ is the m_w th chip of the u th stream and $m_w = (n \bmod L_w)$, $S_u[m_s]$ is the m_s th information symbol of the u th stream and $m_s = \lfloor n/L_w \rfloor$, α_p ,

S_p , and W_p are the scaling factor, the pilot symbol, and the Walsh sequence of the pilot stream, respectively.

The data packet structure of the DSSS system is shown in Fig. 2.

B. Channel Model and Receiver

Fig. 3 shows the receiver structure. It can be seen that at the receiver, the frame head is firstly found by the synchronization algorithm. The receiver then performs coarse Doppler frequency estimation using the preamble and resamples the received signals. An automatic frequency offset controller is adopted to track the frequency offset within a data packet. Then channel estimation and equalization algorithms are applied to the received signals to estimate the transmitted data. Note that since the preamble and the pilot are known to the receiver, both of them can be used for channel estimation. The performance of both the preamble-based and pilot-based channel estimation will be compared by numerical simulations.

We assume that the packet detection and synchronization are perfect. After the resampling operation, the discrete-time signal samples are given by

$$r[n] = \exp(j\theta[n]) \sum_{c=1}^{L_h} x[n - \tau_c] h_c + w[n] \quad (2)$$

where $\theta[n]$ is the phase shift due to the frequency offset, τ_c is the delay of the c th path, L_h is the number of multipath, $h_c = g_c \exp(j\theta_c)$ is the channel impulse response of the c th path, and $w[n]$ is the additive white Gaussian noise (AWGN) with zero mean and variance σ^2 .

C. Automatic Frequency Offset Control (AFC)

The frequency offset $f[m_s]$ is assumed to be constant during one pilot symbol and we utilize the random walk process to model this parameter as

$$f[m_s] = f[m_s - 1] + n_f[m_s], \quad m_s = 1, \dots, N_d \quad (3)$$

with $f[0] = 0$, where $n_f[m_s]$ is additive zero-mean white Gaussian noise with variance σ_f^2 .

After descrambling and despreading with the Walsh code of the pilot symbol, from $r[n]$ in (2) we can obtain an estimate of the m_s th received pilot symbol $\tilde{S}_p[m_s]$. The measurement model of the EKF is given by

$$\begin{aligned} d_{m_s} &= \tilde{S}_p[m_s] S_p^*[m_s] \tilde{S}_p^*[m_s - 1] S_p[m_s - 1] \\ &\approx \exp(j2\pi f[m_s - 1] L_w T_c) + w_d[m_s] \end{aligned} \quad (4)$$

where $(\cdot)^*$ denotes the complex conjugate, T_c is the chip duration, and $w_d[m_s]$ is approximated to be zero-mean Gaussian noise. Based on the state equation (3) and the measurement equation (4), an EKF is applied to track $f[m_s]$, $m_s = 1, \dots, N_d$, within a data packet. Then the carrier frequency offset is compensated from the received samples as

$$\tilde{r}[n] = \exp(-j\tilde{\theta}[n]) r[n] \quad (5)$$

where $\tilde{\theta}[n]$ is an estimation of $\theta[n]$ based on $f[m_s]$ obtained from the EKF.

D. Channel Estimation and Equalization

After the carrier frequency offset estimation and compensation, channel estimation is performed based on the cross-correlation of $\tilde{r}[n]$ in (5) with the local version of the known preamble or pilot sequence. Two channel estimation schemes are considered: a preamble-based method and a pilot-based method.

In the preamble-based method, the channel estimation is based on the following cross-correlation

$$R[\tau] = \frac{1}{L_{pr}} \sum_{n=1}^{L_{pr}} \tilde{r}[n + \tau] s^*[n], \quad 0 \leq \tau \leq \tau_{max} \quad (6)$$

where $s[n]$ is the n th chip of the preamble sequence, τ_{max} is a predefined parameter denoting the maximum channel delay (searching range) supported by the receiver. Note that the actual maximum channel delay is unknown at the receiver and it can be shorter or longer than τ_{max} . In the preamble-based method, channel estimation is performed only once in every data packet.

In contrast to the preamble-based method, channel estimation is performed for each symbol in every data packet. For the m_s th symbol, the channel estimation result of the c th path using the pilot-based method can be expressed as

$$\tilde{h}_c[m_s] = \frac{1}{L_w \alpha_p} S_p^*[m_s] \sum_{n=m_s L_w}^{(m_s+1)L_w-1} \tilde{r}[n + \tau_c] W_p[m_w] C^*[n]. \quad (7)$$

The channel estimates in (7) are smoothed over L_a consecutive symbols to reduce the impact of channel noise by assuming that the phase distortion $\tilde{\theta}[n] - \theta[n]$ caused by the residual frequency offset is very small within L_a symbols. We denote the smoothed channel estimation as $\hat{h}_c[m_s]$, $c = 1, \dots, L_h$.

In the equalization module, the received data streams are first descrambled and despread by a matched filter and resolved into L_h -paths signals with different time delays. The matched filter is equivalent to a series of synchronous coherent combiners. The estimate of the m_s th symbol from the u th data stream associated with the c th path can be represented as

$$\begin{aligned} \tilde{S}_{u,c}[m_s] &= \frac{1}{L_w \alpha_u} \sum_{n=m_s L_w}^{(m_s+1)L_w-1} \tilde{r}[n + \tau_c] W_u[m_w] C^*[n] \\ &= h_c \exp(j\phi_c[m_s]) S_u[m_s] + w_{s,u,c}[m_s] \end{aligned} \quad (8)$$

where $\phi_c[m_s]$ is the phase distortion of the c th path at the m_s th symbol caused by the residual frequency offset after the AFC. To implement the coherent rake receiver for multipath signals, we need to accurately estimate the multipath channel and the phase distortions. The estimated symbol in (8) is multiplied by $\hat{h}_c^*[m_s] \exp(-j\phi_c[m_s])$ and all the L_h resolved signals are combined using the maximal-ratio combining (MRC) method as



$$\hat{S}_u[m_s] = \sum_{c=1}^{L_h} \hat{h}_c^*[m_s] \exp(-j\phi_c[m_s]) \tilde{S}_{u,c}[m_s]. \quad (9)$$

III. SIMULATION RESULTS

TABLE I. PARAMETERS OF THE DSSS SYSTEM

Parameter	Value
L_w	64
$\alpha_1, \dots, \alpha_U$	$\sqrt{1/(U+1)}$
a_p	$\sqrt{1/(U+1)}$
L_{pr}	256
N_d	200
Modulation	QPSK
Sampling rate	500 Hz

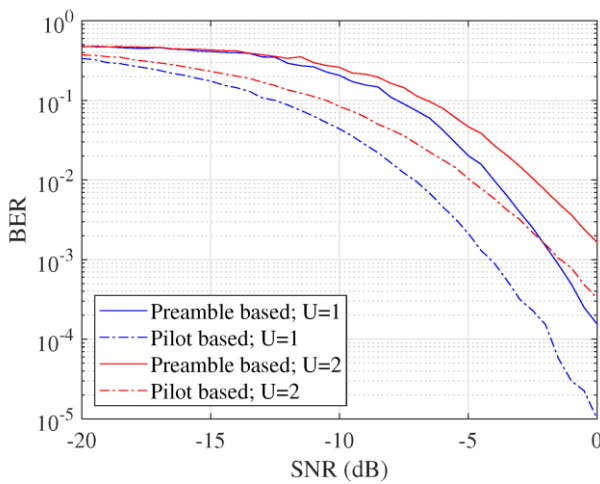


Figure 4. System BER performance with rake receiver.

In this section, we study the performance of the DSSS communication system. The system parameters are summarized in Table I.

A. Channel Estimation

In this subsection we focus on the estimation of the multipath channel and its impact on the DSSS system. To avoid the effect of frequency offset, we assume that it is perfectly removed and the residual frequency offset is zero. For the pilot-based channel estimation we smooth the results over all N_d pilot symbols. In the numerical simulations, we assume that τ_{max} is known to the system.

We simulate a UA channel with 15 paths. The arrival times of all paths follow a Poisson distribution with an average delay of 12.5 ms between two adjacent paths. The amplitudes of the paths are Rayleigh distributed with variances following an exponentially decreasing profile. The ratio of the channel variances between the start and the 200 ms-delay is 3 dB. Note

that the average delay spread of this channel is 200 ms which is longer than the spreading code duration ($64/500 = 128$ ms).

The system BER performance versus the SNR is shown in Fig. 4. The simulation results indicate that the system is reliable to transmit multiple data streams in parallel with both preamble-based and pilot-based channel estimations. The pilot-based channel estimation works even when the channel delay spread is longer than the spreading code duration, which is one of the important contributions of the packet-wide scrambling structure. It is also notable that the pilot-based channel estimation has better BER performance than the preamble-based channel estimation. This is mainly because the pilot uses more chips and energy to perform channel estimation. At low SNR where channel estimation precision is the system bottleneck, pilot-based channel estimation ensures much more accurate results. It is reasonable to predict that with the increase of SNR, the two algorithms should eventually have similar channel estimation precisions, resulting in similar BER performance.

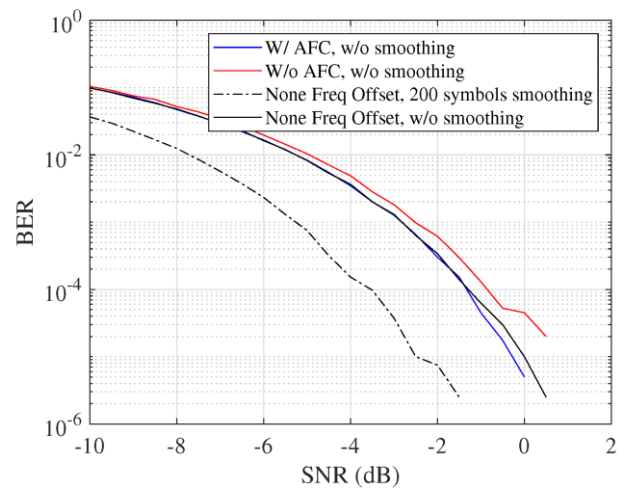


Figure 5. System BER performance with the AFC.

B. Frequency Offset Tracking

In this subsection we utilize the EKF algorithm to track the frequency offset, and analyze the corresponding performance improvement of our DSSS system. In order to focus on the frequency offset tracking, we ignore the effect of multiple paths. Thus, only one path with unknown phase shift θ_1 is assumed. In the simulations, we set $\sigma_f^2 = 0.01$.

Fig. 5 compares the system BER performance with and without utilizing the AFC. As a baseline, we also show the BER performance of the system whose channel has no frequency offset. It can be seen from Fig. 5 that the EKF-based AFC algorithm improves the system performance by around 0.5 dB when the smoothing processing is bypassed. The system BER performance using the AFC is very close to that of the system with no frequency offset. It is also notable that the smoothing processing can bring around 2 dB benefit for the none frequency offset scenario.

Fig. 6 shows the BER performance with various smoothing length for systems with and without the AFC. When the system bypasses the AFC processing, the smoothing operation decreases the BER performance as the phase distortions between two consecutive symbols are not ignorable. However, for the system with the AFC, the channel estimation smoothing operation between two consecutive symbols brings around 1 dB gain. It is worth noting that smoothing with a larger number of symbols improves the system BER performance when the SNR is low, but leads to a worse performance at high SNRs. This is mainly because the residual phase distortions between adjacent symbols are slightly different. At low SNRs, the AWGN is the main factor which limits the channel estimation quality. Thus, smoothing with more symbols improves the channel estimation accuracy. On the other hand, at high SNRs, the difference between the phase distortions plays a decisive role in the smoothing operation. In this case, smoothing with longer signal results is lower channel estimation accuracy.

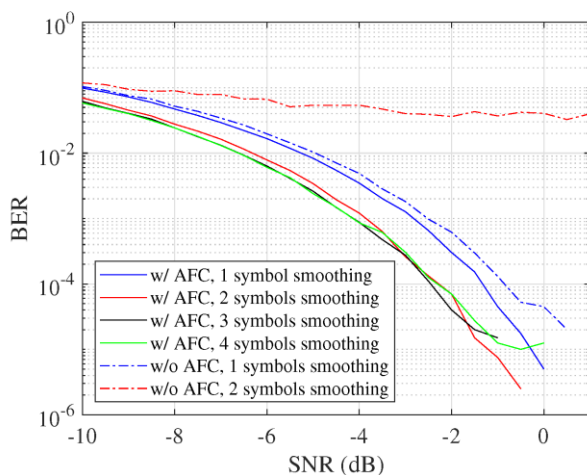


Figure 6. BER performance with various smoothing length.

IV. CONCLUSIONS AND FUTURE WORKS

We have performed an initial feasibility study of a packet-wide scrambled DSSS based underwater acoustic communication system in this paper. In the next stage we will investigate the pilot sequence optimization, including the power allocation between the data streams and the pilot stream, to achieve a desired tradeoff between the system data rate and error probability.

REFERENCES

- [1] M. Stojanovic, J. G. Proakis, J. A. Rice, and M. D. Green, "Spread spectrum underwater acoustic telemetry," in Proc. MTS/IEEE OCEANS, 1998, vol. 2, pp. 650-654.
- [2] J. G. Proakis, Digital Communications. New York, NY, USA: McGraw-Hill, 2001.
- [3] H.-W. Lee, E.-H. Jeon, T.-I. Kwon, K.-M. Kim, D.-W. Lee, and T.-D. Park, "Design of orthogonal code for covert underwater acoustic communication," in Proc. MTS/IEEE OCEANS, Apr. 2016, pp. 1-4.
- [4] T. C. Yang and W. Yang, "Interference suppression for code-division multiple-access communications in an underwater acoustic channel," J. Acoust. Soc. Amer., vol. 126, no. 1, pp. 220-228, 2009.
- [5] D. B. Kilfoyle and A. B. Baggeroer, "The state of the art in underwater acoustic telemetry," IEEE J. Ocean. Eng., vol. 25, no. 1, pp. 4-27, Jan. 2000.
- [6] E. Calvo and M. Stojanovic, "Efficient channel-estimation-based multiuser detection for underwater CDMA systems," IEEE J. Ocean. Eng., vol. 33, no. 4, pp. 502-512, Oct. 2008.
- [7] F. Qu, X. Qin, L. Yang, and T. C. Yang, "Spread-spectrum method using multiple sequences for underwater acoustic communications," IEEE J. Ocean. Eng., vol. 43, no. 4, pp. 1215-1226, Oct. 2018.
- [8] T. C. Yang and W. Yang, "Performance analysis of direct-sequence spread-spectrum underwater acoustic communications with low signal-to-noise-ratio input signals," J. Acoust. Soc. Amer., vol. 123, no. 2, pp. 842-855, 2008.
- [9] T. C. Yang and W. Yang, "Low probability of detection underwater acoustic communications using direct-sequence spread spectrum," J. Acoust. Soc. Amer., vol. 124, no. 6, pp. 3633-3647, 2008.
- [10] J. Ling, H. He, J. Li, W. Roberts, and P. Stoica, "Covert underwater acoustic communications," J. Acoust. Soc. Amer., vol. 128, no. 5, pp. 2898-2909, 2010.
- [11] E. M. Sozer, J. G. Proakis, M. Stojanovic, J. A. Rice, A. Benson, and M. Hatch, "Direct sequence spread spectrum based modem for underwater acoustic communication and channel measurements," in Proc. MTS/IEEE OCEANS, 1999, vol. 1, pp. 228-233.
- [12] M. Stojanovic and L. Freitag, "Multichannel detection for wideband underwater acoustic CDMA communications," IEEE J. Ocean. Eng., vol. 31, no. 3, pp. 685-695, Jul. 2006.
- [13] M. Stojanovic, "Hypothesis-feedback equalization for direct-sequence spread-spectrum underwater communications," in Proc. MTS/IEEE OCEANS, Providence, RI, USA, 2000, pp. 123-129.
- [14] F. Blackmon, E. M. Sozer, M. Stojanovic, and J. Proakis, "Performance comparison of RAKE and hypothesis feedback direct sequence spread spectrum techniques for underwater communication applications," in Proc. MTS/IEEE OCEANS, 2002, vol. 1, pp. 594-603.
- [15] A. Tadayon and M. Stojanovic, "Low-complexity superresolution frequency offset estimation for high data rate acoustic OFDM systems," IEEE J. Ocean. Eng., vol. 44, no. 4, pp. 932-942, 2019.
- [16] S.-M. Hwang, M. Yu, and L. Yang, "A low complexity carrier recovery and frequency estimation algorithm for Iridium handset system," in Proc. IEEE Wireless Commun. Network. Conf., vol. 3, pp. 1208-1211, 1999.
- [17] M. K. Simon, "Dual-pilot tone calibration technique," IEEE Trans. Veh. Technol., vol. 35, pp. 63-70, May 1986.
- [18] Y. E. Wang and T. Ottosson, "Cell search in W-CDMA," IEEE J. Select. Areas Commun., vol. 18, pp. 1470-1482, Aug. 2000.

